7 January 2000

ELSEVIER

Chemical Physics Letters 316 (2000) 13–18

CHEMICAL PHYSICS LETTERS

www.elsevier.nl/locate/cplett

Controlling single-wall nanotube diameters with variation in laser pulse power

A.C. Dillon, P.A. Parilla, J.L. Alleman, J.D. Perkins, M.J. Heben *

National Renewable Energy Laboratory, 1617 Cole Blvd., Golden CO, 80401-3393, USA

Received 23 April 1999; in final form 11 October 1999

Abstract

We demonstrate that laser peak pulse power can be employed to tune carbon single wall nanotube (SWNT) diameters. The production of SWNTs was investigated at room temperature and at 1200°C. The diameters were shifted to smaller sizes in both cases as the pulse power was increased. SWNT size distributions and yields were studied with Raman spectroscopy and transmission electron microscopy. The evolution of the material quality with laser energy parameters offers insight in to SWNT formation mechanisms. These studies should aid in the development of methods for the rational control of SWNT growth.

1. Introduction

Since SWNTs were first discovered in 1991 [1], several advances in synthesis have led to the production of tubes in larger quantities and higher purities. The electric arc technique first generated macroscopic quantities of tubes [2,3], and higher SWNT densities were obtained when 532 nm laser pulses were directed onto metal-doped carbon targets [4]. The development of new catalysts for use in the electric arc resulted in higher quantities of SWNTs [5], and SWNTs have also been produced by decomposing CO [6], CH_4 [7] or benzene [8] on metal catalyst particles. Most of the laser-based synthesis experiments to date have followed the pioneering work of Guo et al. [4] and Thess et al. [9] by utilizing laser pulses shorter than ~ 10 ns and heating the target with an external furnace. SWNT synthesis with continuous wave (cw) irradiation was first shown using a Nd:YAG laser operating at 1064 nm [10], and then with a CO_2 laser operating at 10.6 μm [11]. Both of these efforts achieved SWNT growth without the use of an external furnace. A recent study compares the yield for SWNTs using 20 ms, 10.6 μm pulses from a CO_2 laser to that with short (5–7 ns), 532 nm pulses from a Nd:YAG laser [12].

A variety of different synthetic methods provide conditions which lead to SWNT growth. Most research to date has focused on whether or not tubes could be made at all and on determining the essential conditions for maximizing production rate and purity. Although a considerable amount has been learned, much work remains before SWNT growth can be fully controlled. In particular, one would like to be able to fabricate samples of specific tubes, and perhaps even generate 'phase-pure' samples having only one type of tube. SWNT diameters are currently

* Corresponding author. Fax: +1-303-384-6655; e-mail: mikeh@nrel.gov

0009-2614/00/$ - see front matter
PII: S0009-2614(99)01259-2

measured but not controlled, and size distributions differ widely depending on synthesis conditions. Rational control over SWNT size distributions would enable the study of physical and chemical phenomena in tailored samples. Such samples are required since many of the potential applications envisioned for SWNTs are dependent on the specifics of chirality and diameter [13,14].

Tuning of SWNT diameters by varying the target temperature was recently demonstrated by Bandow et al. [15]. With a two-pulse laser sequence, the diameter of the dominant tube shifted from 1.0 to 1.2 nm as the temperature was increased from 850 to 1050°C. In this letter, we describe how laser energy parameters can be varied at constant temperature to tune SWNT diameters from ~1.1 to 1.4 nm. SWNT syntheses were performed at both room temperature and 1200°C with Nd:YAG laser pulses with durations between the short-pulse and long-pulse limits that have been previously explored. Raman spectroscopy showed that the predominant SWNT diameter can be varied from approximately that of an (8,8) to that of a (10,10) tube when laser pulse energy parameters are varied appropriately. Significant populations of non-armchair tubes may also be produced. The gas phase population of carbon fragments are precursors for SWNT formation, and the size distribution and density of these fragments are altered by the laser pulse power. The ambient temperature determines if these fragments have sufficient thermal energy to assemble into tubes. Since the temperature for carbon vaporization is much higher than required for metal vaporization, the metal species are assumed to be atomically dispersed in the gas phase for all laser runs. Thus, the work focuses on the role of the carbon fragments thereby providing new insight into the mechanisms of SWNT formation. SWNT diameter tuning by variation in laser pulse parameters is demonstrated for the first time.

2. Experimental

For room temperature experiments, 4 μm graphite powder was doped with 0.6 at % each of Co and Ni powder and mixed with 50 wt % polyethylene glycol (PEG). The mixture was formed into targets by pressing in a 2.9 cm dye to 700 kg/cm^2 for 3 min, and heating in argon to 1000°C for 4 h. The targets were supported with a tantalum holder in a 3.8 cm quartz tube which was purge-cycled with Ar three times between 1 and 750 torr while the target was baked with an infrared lamp. The output of a Control Q-switched Nd:YAG (1064 nm) laser was focused to ~0.86 mm^2 and rastered across the target. The laser generated an average power of up to 3.5 kW/cm^2 in continuous-wave (cw) mode, and a peak power ranging from 0.2 to 3.5 MW/cm^2 when pulsed. Variation of the peak power density was achieved through variation in the pulse width and frequency as shown in Table 1. Runs at 1200°C were performed using a Molectron Nd:YAG (1064 nm) that could be Q-switched to produce ~10 ns pulses, or operated in a 'long-pulse' mode in which the laser was free-running during the ~450 ns light pulse from the flash lamps. Targets for these experiments were prepared by pressing the Co–Ni–C powder to 1400 kg/cm^2 in a 2.9 cm dye without either the addition of PEG or subsequent annealing. Laser exposures were performed with Ar flowing at 50 sccm and a pressure of 500 torr. The materials were collected after each experiment and examined by TEM. Raman spectroscopy was performed using a 50 mW Argon ion laser operating at 488nm with a resolution of ~0.6

Table 1
Relationship between the operating characteristics of the Control Corporation Q-switched Nd:YAG laser

Pulse width (ns)	Peak power (MW/cm^2)	Average power (kW/cm^2)	Pulse frequency (kHz)
175	3.5	1.8	3
250	1.5	2.3	6
300	0.9	2.8	10
575	0.2	3.0	24

nm (4–6 cm^{-1}) across the entire range of interest. Calibration was performed with Oriel spectral lamps.

3. Results and discussion

Raman spectroscopy in the region of the radial breathing modes reveals changes in the SWNT size distributions as a function of laser pulse power for tubes produced at room temperature (Fig. 1). For purposes of discussion, we follow Rao et al. [16] in assigning Raman signals to specific tubes. Focussing first on the data for material produced with 575 ns pulses (Fig. 1a), two distinct signals at 183 and 202 cm^{-1} are observed. The first signal is dominant and can be assigned to the radial breathing mode of the (9,9) armchair tube. The second signal is $\sim$50% of the intensity of the (9,9) feature and lower in frequency than expected for (8,8) tubes (206 cm^{-1}). However, we still assign this feature to the (8,8) tube through consideration of stability arguments [17] and the instrumental limitations. The material was produced at the maximum average power output available with 575 ns pulses (3.0 kW/cm^2) at 24 kHz so the pulse power was 0.2 MW/cm^2 (Table 1). Fig. 1b shows the Raman data for material generated with 300 ns pulses. The 300 ns pulses were generated at an average power of 2.8 kW/cm^2 and a frequency of 10 kHz, so the peak pulse power is 0.9 MW/cm^2. The (9,9) feature is no longer strongly dominant, and a new feature found at 165 cm^{-1} corresponds to the appearance of (10,10) tubes [16]. The (8,8) and (9,9) signals exhibit equal intensities which are twice as strong as the signal from the (10,10) tubes. Overall, the SWNT diameter distribution is shifted to smaller tubes in comparison to the material prepared with a pulse power of 0.2 MW/cm^2. The trend leading to smaller SWNTs with higher pulse powers continues when 250 ns pulses are employed at an average power of 2.3 kW/cm^2 corresponding to a peak power of 1.5 MW/cm^2 (Fig. 1c). Although the concentration of tubes was only $\sim$4% [10], a Raman signal associated with the radial breathing mode of (8,8) tubes can be clearly discerned above the background. There is also some indication of a (9,9) signal, but the distribution is centered very near to the diameter of the (8,8) tube. Raman spectroscopy was also performed on material generated with a peak power of 3.5 MW/cm^2 but no SWNT modes were observed. The Raman data of Fig. 1 show that the fragment distributions prepared by higher pulse powers can result in the formation of smaller tubes. However, the reduction of intensity of the radial breathing mode signals with increasing pulse power indicates that the overall efficiency of tube formation is decreased.

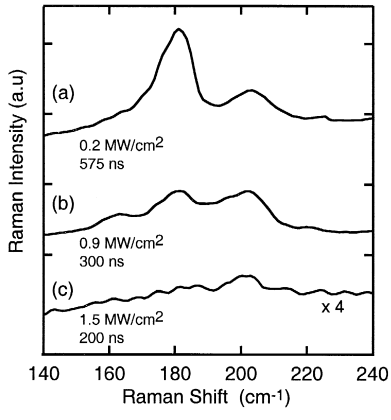

Fig. 1. Raman spectra of the radial breathing modes of single-wall carbon nanotubes. The materials were generated at room temperature with 1064 nm laser pulses with pulse powers of (a) 0.2 MW/cm^2, (b) 0.9 MW/cm^2, and (c) 1.5 MW/cm^2. The pulse width is noted in the figure, and the laser repetition rates and average powers are provided in the text and Table 1.

The nature of the ablated/vaporized carbon species which are not incorporated into SWNTs can be probed with Raman spectroscopy in the range of 1200 to 1800 cm^{-1}. The spectrum from the initial target material is shown for comparison in Fig. 2a. The major sharp feature at 1589 cm^{-1} is due to the fundamental E_{2g} mode of graphite [18] and is expected for the 4 μm graphite crystallites in the target. The minor broader band at $\sim$1360 cm^{-1} is related to the structural disorder of the sp^2 carbon at edges and defects of the graphite particles and is referred to as the 'D band' [18,19]. Both the D and the E_{2g} bands are broader in the 3.5 MW/cm^2 material (Fig. 2b), and their intensity is approximately equal. Graphite modes broaden with decreasing domain size [20,21], and the D band increases in intensity with decreasing crystal size below $\sim$1 μm [18,22]. When the domain size is about 10 nm, the two Raman features have approximately equal inten-

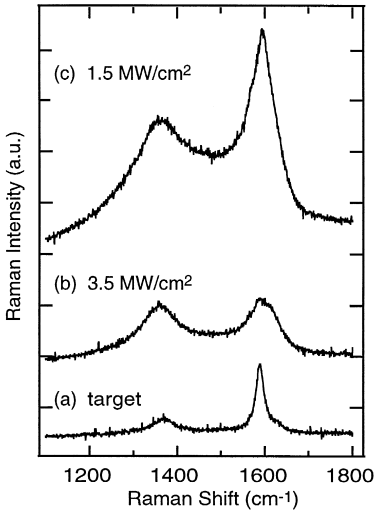

Fig. 2. Raman spectra of (a) the initial target, (b) soot produced with 1064 nm laser pulses with a pulse power of 3.5 MW/cm^2, (c) soot produced with 1064 nm laser pulses with a pulse power of 1.5 MW/cm^2. Related data are presented in Table 1.

sities. This is the case for the data in Fig. 2b. However, the sharp feature at 1589 cm^{-1} indicates the additional presence of ~ 4 μm graphite particles from the target. Thus, the 3.5 MW/cm^2 soot contains both nano-crystallites formed by vaporization and condensation, as well as target particles ejected by ablation [10]. The SWNT Raman features begin to appear in the spectrum of the material produced at a pulse power of 1.5 MW/cm^2 (Fig. 2c). The curvature of the SWNTs lifts the degeneracy of the E_{2g} mode in single crystal graphite and the accompanying resonant enhancement gives rise to the well-known sharp feature at 1593 cm^{-1} with a shoulder at 1567 cm^{-1} [16]. The D band is still of approximately the same width and intensity as the nanocrystalline graphite E_{2g} mode underlying the SWNT modes. The overall intensity is increased due to the increase in the fraction of the nanocrystalline carbon and the decrease in the fraction of the ablated target material. The appearance of the sharp feature at 1593 cm^{-1} indicates that the additional heating brought about by the higher average power and pulse repetition rate (Table 1) allows the small fragments to begin to assemble into tubes.

Any given carbon fragment distribution prepared in the gas phase by laser irradiation can condense into either SWNTs or other carbonaceous solids. Pulsed light delivered at room temperature forms tubes with relatively low efficiency in comparison to cw irradiation at similar average powers [10]. This is true since cw light heats the target and the laser plume more than does pulsed light. The heating provides thermal energy to allow fragments to assemble into SWNTs. This energy is normally provided by an external furnace when short laser pulses are employed. When external heating is not supplied to facilitate annealing, a large percentage of pulse-produced gas-phase fragments are quenched into non-SWNT structures. The density of tubes is increased at the lower pulse powers because both ablation is decreased and the repetition rates is higher so the irradiation begins to behave more like the cw case [10].

The characteristics of the Control laser are such that pulse width, pulse frequency, and peak pulse power cannot be independently controlled. Consequently, it is difficult to decouple the effects of peak pulse power from the target heating produced at the higher pulse repetition rates. In an effort to separate these parameters, samples were generated using a Molectron Nd:YAG laser that could be operated in either Q-switched (10 ns) or long-pulse (450 ns) modes. The pulse repetition rate was fixed at 10 Hz and these experiments were performed with an external furnace surrounding the target at a temperature of 1200°C. Fig. 3 shows Raman spectra in the radial breathing mode region for SWNT materials produced with three different types of laser pulses. Spectrum 3a shows data from material produced at an average power of 200 W/cm^2 in long-pulse mode where the pulse power is 45 MW/cm^2. Three signals are present at 164, 177 and 182 cm^{-1} consistent with populations of (10,10), (16,0), and (9,9) tubes [16]. Much weaker signals at 193 and 202 cm^{-1} may also be discerned. The Raman spectrum is dramatically shifted to higher frequencies corresponding to smaller tubes when the average power is maintained at 200 W/cm^2 but the laser is Q-switched to yield a pulse power of 2 GW/cm^2 (Fig. 3b). The 164 cm^{-1} peak is no longer observed, and the signals at 177 and 182 cm^{-1} are significantly reduced in intensity. Two new strong bands found at 202 and 193 cm^{-1} can be associated with (8,8) tubes and a slightly larger non-armchair tube such as the (14,0) tube, respectively.

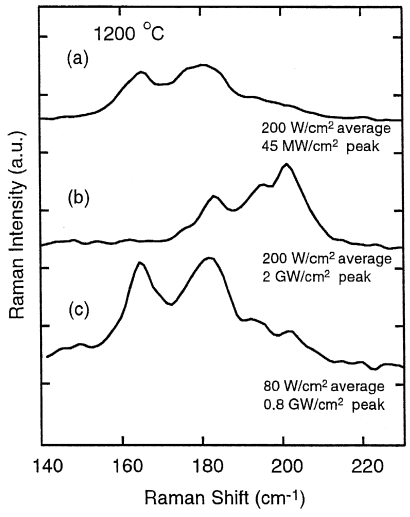

Fig. 3. Raman spectra of the radial breathing modes of single-wall carbon nanotubes. The materials were generated at 1200°C with 1064 nm laser pulses at 10 Hz and (a) 200 W/cm^2 average power corresponding to 45 MW/cm^2 in 450 ns, (b) 200 W/cm^2 average power corresponding to 2 GW/cm^2 peak power in 10 ns, and (c) 80 W/cm^2 average power corresponding to 0.8 GW/cm^2 peak power in 10 ns.

The data are consistent with the shift to smaller tubes seen with increasing peak pulse power in the experiments at room temperature. However, with the Molectron laser, the comparison can be made at different peak powers when the average power and pulse repetition rate are the same. The shift to smaller tubes is clearly due to the increased pulse power. The point is proven further by considering the size distribution of SWNTs when the average power, and thus the pulse power, are reduced while the pulse width and repetition rate are held constant. Fig. 3c shows the radial breathing modes for SWNTs produced at an average power of 80 W/cm^2 and a 10 ns pulse width so the peak power is 0.8 GW/cm^2. The SWNT size distribution is shifted to larger values in comparison to the distribution obtained at a peak power of 2 GW/cm^2, and is in fact similar to the size distribution found at an average power of 200 W/cm^2 in the long-pulse mode. Two major features are present at 164 and 182 cm^{-2} as expected for (10,10) and (9,9) tubes, and weaker modes at 193 and 202 cm^{-1} are also seen.

Several studies have explored the carbon fragment size distributions produced with short laser pulses ($\sim$10 ns) [23–25]. A general conclusion is that higher laser peak pulse powers produce smaller gas-phase carbon fragments. For instance, C_1 and C_3 fragments are the only products when 10 ns, 1064 nm pulses were directed at a pure graphite target at a peak power of 230 MW/cm^2, while a lower peak power of 80 MW/cm^2 produced a wide distribution of fragments spanning from C_3 to C_{15} with C_{11} predominating [23]. The same general behavior is seen for 532 nm pulses [24]. The lower peak powers remove relatively large pieces of graphite, but cannot readily break the graphene sheets into smaller fragments. In contrast, the higher peak powers deliver sufficient energy in a short enough time to break nearly all carbon–carbon bonds [25]. The smaller fragments generated by the higher peak pulse powers are evidently better suited for assembly and/or incorporation into smaller tubes. In contrast to the data from the room temperature runs, the efficiency of tube assembly can be fairly high when the thermal energy necessary for assembly is supplied by an external furnace. No SWNTs were found after irradiation of room temperature targets at a pulse power of 3.5 MW/cm^2, and a maximum of $\sim$30% was found in the soot produced at 0.2 MW/cm^2 [10]. In contrast, the SWNT densities are relatively high between $\sim$15 and 30% in each of the samples used in Fig. 3.

The pulse powers generated by the Molectron are much higher than the peak powers used in the carbon fragment studies discussed above, and the pulse powers generated by the Control laser are much lower. However, the shift in SWNT diameter towards smaller tubes with increasing pulse power is seen with both lasers. The porosity and thermal conductivity of the target effect how the arriving laser energy is dissipated in the target. The porous targets used for the Control laser experiments enable the target surface temperature to be higher because the energy cannot be easily dissipated. Porous targets were necessary with this high-repetition rate laser since very little soot was produced and the target was simply heated when dense targets were employed. In contrast, dense targets were required when high power Molectron pulses were utilized since only ablated target particles were generated from porous targets. There is clearly an interplay between target parameters, energy delivery parameters, and

thermal parameters which control the yield as well as the diameter distribution of SWNTs. For efficient and controlled SWNT growth it is important to operate in a regime in which the target is vaporized rather than ablated.

4. Conclusion

We have demonstrated that SWNT diameter distributions can be tuned through variation in laser pulse power. The production of SWNTs was investigated at room temperature with a porous target, and at 1200°C with a dense target. The tube diameters were shifted to smaller sizes with increasing pulse power in both cases. The SWNT size distributions and yields were studied with Raman spectroscopy and transmission electron microscopy, and the evolution of the material quality with laser energy parameters was investigated. The smaller fragments generated by the higher peak pulse powers result in the formation of smaller tubes. But the yield for small tubes is low unless thermal energy for assembling is provided by an external furnace. The study offers a unique view of SWNT formation mechanisms and should aid in the development methods for the rational control of SWNT growth.

Acknowledgements

This work was funded by the US Department of Energy Hydrogen Program under contract number DE-AC36-99GO10337.

References

[1] S. Iijima, Nature 354 (1991) 56.
[2] D.S. Bethune, C.-H. Kiang, M.S. de Vries, G. Gorman, R. Savoy, J. Vasquez, R. Beyers, Nature 363 (1993) 605.
[3] S. Iijima, T. Ichihashi, Nature 363 (1993) 603.
[4] T. Guo, P. Nikolaev, A. Thess, D.T. Colbert, R.E. Smalley, Chem. Phys. Lett. 243 (1995) 49.
[5] C. Journet, W.K. Maser, P. Bernier, A. Loiseau, M. Lamy de la Chapells, S. Lefrant, P. Deniard, R. Lee, J.E. Fischer, Nature 388 (1997) 756.
[6] H. Dai, A.G. Rinzler, P. Nikolaev, A. Thess, D.T. Colbert, R.E. Smalley, Chem. Phys. Lett. 260 (1996) 471.
[7] J. Kong, A. Cassell, H. Dai, Chem. Phys. Lett. 292 (1998) 567.
[8] H.M. Cheng, F. Li, G. Su, H.Y. Pan, L.L. He, X. Sun, M.S. Dresselhaus, Appl. Phys. Lett. 72 (1998) 3282.
[9] A. Thess, R. Lee, P. Nikolaev, H. Dai, P. Pitit, J. Robert, C. Xu, Y.H. Lee, S.G. Kim, A.G. Rinzler, D.T. Colbert, G.E. Scuseria, D. Tomanek, J.E. Fischer, R.E. Smalley, Science 273 (1996) 483.
[10] A.C. Dillon, P.A. Parilla, K.M. Jones, G. Riker, M.J. Heben, Mater. Res. Soc. Conf. Proc. 526 (1998) 403.
[11] W.K. Maser, E. Munoz, A.M. Benito, M.T. Martinez, G.F.d.l. Fuente, Y. Maniette, E. Anglaret, J.-L. Sauvajol, Chem. Phys. Lett. 292 (1998) 587.
[12] M. Yudasaka, F. Kokai, K. Takahashi, R. Yamada, N. Sensui, T. Ichihashi, S. Iijima, J. Phys. Chem. B 103 (1999) 3576.
[13] B.I. Yakobson, R.E. Smalley, Am. Sci. 85 (1997) 324.
[14] A.C. Dillon, K.M. Jones, T.A. Bekkedahl, C.H. Kiang, D.S. Bethune, M.J. Heben, Nature 386 (1997) 377.
[15] S. Bandow, S. Asaka, Y. Saito, A.M. Rao, L. Grigorian, E. Richter, P.C. Eklund, Phys. Rev. Lett. 80 (1998) 3779.
[16] A.M. Rao, E. Richter, S. Bandow, B. Chase, P.C. Eklund, K.A. Williams, S. Fang, K.R. Subbaswamy, M. Menon, A. Thess, R.E. Smalley, G. Dresselhaus, M.S. Dresselhaus, Science 275 (1997) 187.
[17] A. Thess, R. Lee, P. Nikolaev, H. Dai, P. Pitit, J. Robert, C. Xu, Y.H. Lee, S.G. Kim, A.G. Rinzler, D.T. Colbert, G.E. Scuseria, D. Tomanek, J.E. Fischer, R.E. Smalley, Science 273 (1996) 483.
[18] Y. Wang, D.C. Alsmeyer, R.L. McCreedy, Chem. Mater. 2 (1990) 557.
[19] P.C. Eklund, J.M. Holden, R.A. Jishi, Carbon 33 (1995) 959.
[20] M. Nakamizo, R. Kammereck, P.L. Walker, Carbon 12 (1974) 259.
[21] J.M. Holden, P. Zhou, X.-X. Bi, P.C. Eklund, S. Bandow, R.A. Jishi, K. Das Chowdhury, G. Dresselhaus, M.S. Dresselhaus, Chem. Phys. Lett. 220 (1994) 186.
[22] F. Tunistra, J.L. Koenig, J. Chem. Phys. 53 (1970) 1126.
[23] J.J. Gaumet, A. Wakisaka, Y. Shimizu, Y. Tamori, J. Chem. Soc. Faraday Trans. 89 (1993) 1667.
[24] A. Wakisaka, J.J. Gaumet, Y. Shimizu, Y. Tamori, H. Sato, K. Tokumaru, J. Chem. Soc. Faraday Trans. 89 (1993) 1001.
[25] Y. Iida, E.S. Yeung, Appl. Spectrosc. 48 (1994) 945.